MARTIN MARIETTA ENERGY SYSTEMS LIBRARIES

3 4456 0279956 8

ORNL/TM-10222

ornl

OAK RIDGE
NATIONAL
LABORATORY

MARTIN MARIETTA

Evaluation of Magnetic Coordinates in Finite-Beta, Asymmetric Plasmas

C. O. Beasley
J. A. Rome
S. E. Attenberger
S. P. Hirshman

OAK RIDGE NATIONAL LABORATORY
CENTRAL RESEARCH LIBRARY
CIRCULATION SECTION
4500N ROOM 175
LIBRARY LOAN COPY
DO NOT TRANSFER TO ANOTHER PERSON
If you wish someone else to see this report, send in name with report and the library will arrange a loan.

OPERATED BY
MARTIN MARIETTA ENERGY SYSTEMS, INC.
FOR THE UNITED STATES
DEPARTMENT OF ENERGY

Printed in the United States of America. Available from
National Technical Information Service
U.S. Department of Commerce
5285 Port Royal Road, Springfield, Virginia 22161
NTIS price codes—Printed Copy: A03; Microfiche A01

This report was prepared as an account of work sponsored by an agency of the United States Government. Neither the United States Government nor any agency thereof, nor any of their employees, makes any warranty, express or implied, or assumes any legal liability or responsibility for the accuracy, completeness, or usefulness of any information, apparatus, product, or process disclosed, or represents that its use would not infringe privately owned rights. Reference herein to any specific commercial product, process, or service by trade name, trademark, manufacturer, or otherwise, does not necessarily constitute or imply its endorsement, recommendation, or favoring by the United States Government or any agency thereof. The views and opinions of authors expressed herein do not necessarily state or reflect those of the United States Government or any agency thereof.

ORNL/TM-10222
Dist. Category UC-20 g

Fusion Energy Division

EVALUATION OF MAGNETIC COORDINATES IN FINITE-BETA, ASYMMETRIC PLASMAS

C. O. BEASLEY
J. A. ROME
S. E. ATTENBERGER
S. P. HIRSHMAN

DATE PUBLISHED — November 1987

Prepared by the
OAK RIDGE NATIONAL LABORATORY
Oak Ridge, Tennessee 37831
operated by
MARTIN MARIETTA ENERGY SYSTEMS, INC.
for the
U.S. DEPARTMENT OF ENERGY
under contract DE-AC05-84OR21400

MARTIN MARIETTA ENERGY SYSTEMS LIBRARIES
3 4456 0279956 8

CONTENTS

ABSTRACT v

1 INTRODUCTION 1

2 CALCULATION OF B IN BOOZER COORDINATES 2

3 CALCULATION OF REAL-SPACE COMPONENTS OF B 3

4 PROGRAM DESCRIPTION AND ASSOCIATED CODES OF MAGC1 5

4.1 INPUT 5

4.2 OUTPUT 7

4.3 SUBSIDIARY CODES 8

5 EXAMPLE: FINITE-β ATF 9

6 CONCLUSION 13

REFERENCES 14

ABSTRACT

Analytical and numerical stability or transport calculations for toroidal plasmas are facilitated by using flux coordinates in which the magnetic field lines are straight. A published method for obtaining these magnetic coordinates, or more specifically the Fourier components of the magnetic field in this coordinate system, has existed for a vacuum magnetic field. A procedure for calculating these components for a finite-β plasma equilibrium, however, has not previously been available. (Here, β is the ratio of plasma pressure to magnetic pressure.) In this report, we describe such a procedure, in which we start with an arbitrary-β magnetic equilibrium for which nested toroidal flux surfaces exist and obtain the Fourier components of the magnetic field in straight-line magnetic coordinates. We describe the various numerical procedures, referring to published documentation where needed. We then document the codes involved and apply them to a specific toroidally nonsymmetric, finite-β plasma.

1 INTRODUCTION

Stability and transport calculations often require input of magnetic field components in a straight-line magnetic coordinate system. In particular, calculations of plasma transport coefficients for a three-dimensional (3-D), finite-β plasma of arbitrary geometrical shape by use of a numerical method described by Hirshman et al. [1] require such input. Specifically, one must input spectral components of B^{-1}, B_ζ/B^2, B_θ/B^2, and $\sqrt{g}$, where (B_ζ, B_θ) are the covariant components and B is the magnitude of the magnetic field $\mathbf{B}$ in Boozer coordinates [2] (described in Sect. 2) and where $\sqrt{g}(\Psi)$ is the Jacobian; Ψ, the "radial" coordinate in magnetic flux coordinates, is the toroidal magnetic flux inside a given flux surface.

In this report, we describe a numerical method for obtaining these magnetic field spectra in a straight-line coordinate system, starting with the real-space components $\mathbf{B}(R, \phi, Z)$. Here, $\mathbf{B}$ is the solution of $\nabla p = \mathbf{j} \times \mathbf{B}$ and is obtained from a 3-D magnetohydrodynamic (MHD) equilibrium code. In particular, we show how the MHD equilibrium obtained from MOMCON [3], or its more accurate version, VMEC [4], can be used to obtain these straight-line magnetic flux coordinates, as well as the appropriate magnetic field components in these coordinates. These equilibrium codes output the real-space spectral components of R, Z, and λ, where λ is a renormalization parameter that is used to ensure a rapidly convergent Fourier series for the spatial coordinates (R, Z). A subroutine is then needed to calculate the real-space components of $\mathbf{B}(R, \phi, Z)$ from the output of the MHD equilibrium code. Finally, using this $\mathbf{B}(R, \phi, Z)$, we employ a method developed by Rome and Fowler [5] to calculate the straight-line coordinates for this magnetic field, as well as the Fourier components of B^{-1} and B^{-2} in that coordinate system. A flow chart of the method is given here.

FLOW CHART

Specify Plasma Boundary
(from vacuum magnetic field
or output of any other MHD
equilibrium code)

$\Downarrow$

Obtain Finite-β Equilibrium
VMEC

$\Downarrow$

Transform to Boozer Coordinates
MAGC1

$\Downarrow$

Output Fourier Components in Boozer Coordinates
$B_{nm}, B^{-1}_{nm}, B^{-2}_{nm}, R_{nm}, Z_{nm}, (\phi - \phi_{\text{Boozer}})_{nm}$

Section 2 reviews the method used by Boozer and his colleagues to transform to straight-line (Boozer) coordinates and describes the code (MAGC1) to implement the calculations. Section 3 describes the algorithm to calculate $\mathbf{B}(R, \phi, Z)$ from VMEC or MOMCON output. The differences between MOMCON and VMEC are discussed, and a method for converting MOMCON output to VMEC output is described. Section 4 discusses input/output from MAGC1, as well as code availability. Included with this are subsidiary codes related to input/output. Section 5 shows a sample calculation, and Sect. 6 provides a conclusion.

2 CALCULATION OF B IN BOOZER COORDINATES

The method of Rome and Fowler is described in detail in ref. 5. However, for completeness, we will review the salient points needed to describe its application to the present problem. The method calculates $B(\chi)$, where $\chi = \int \mathbf{B} \cdot d\ell$ is the coordinate along the magnetic field. The magnetic coordinates are defined by

$$\mathbf{B} = \frac{1}{2\pi} \nabla\Psi \times \nabla\theta_o \qquad \text{(contravariant)} \ , \tag{1}$$

$$= \nabla\chi + \hat{\beta}\ \nabla\psi \qquad \text{(covariant)} \ . \tag{2}$$

The coordinate θ_o labels the field line and is constant along a field line, and $\Psi = 2\pi\psi$ is the toroidal flux. These coordinates are related to the toroidally (ϕ) and poloidally (θ) periodic flux coordinates by the relations

$$\chi = g(\psi)\phi + I(\psi)\theta \ , \tag{3}$$

$$\theta = \theta_o + \iota(\psi)\phi \ , \tag{4}$$

where ι is the rotational transform.

A requirement for successful application of the method is the accurate computation of $\mathbf{B}(R, \phi, Z)$ for any (R, ϕ, Z). Since the real-space Fourier components (R_{mn}, Z_{mn}) of (R, Z) are output only on a discrete set of flux surfaces by the MHD equilibrium code MOMCON [3] or VMEC [4], a splining technique (discussed in Sect. 3) is needed to obtain (R_{mn}, Z_{mn}) on an arbitrary flux surface. To follow a field line, the components $\mathbf{B}$ need to be calculated accurately. Also, the values of $g(\psi)$, $I(\psi)$, and $\iota(\psi)$ are needed, where $(2\pi/\mu_0)g(\psi)$ and $(2\pi/\mu_0)I(\psi)$ are the total poloidal current outside and total toroidal current inside a flux surface, respectively, in mks units. Accuracy of these quantities can be verified in the graphic output by observing if the positions of the peaks of the $m = 0$ Fourier amplitudes calculated by MAGC1 coincide with the toroidal harmonic points $\omega_{n0} = n/g + \iota I$, which are plotted on the same output. [See, for example, Figs. 3(a) and 3(d)]. Here, ω_{nm} is the Fourier transform frequency resulting from Fourier decomposition along χ: $B(\chi) = \sum_{n,m} [a_{nm} \exp(i\omega_{nm}\chi)]$. Since these locations depend on $\hat{\beta}$ through g, I, and ι, this test is quite sensitive.

The various poloidal and toroidal harmonics, $(B_{\text{Boozer}})_{mn}$, $(B^{-1}_{\text{Boozer}})_{mn}$, $(B^{-2}_{\text{Boozer}})_{mn}$, $(R_{\text{Boozer}})_{mn}$, $(Z_{\text{Boozer}})_{mn}$, and $(\phi - \phi_{\text{Boozer}})_{mn}$, are then obtained by the method discussed in ref. 3.

3 CALCULATION OF REAL-SPACE COMPONENTS OF B

For finite-β plasmas, the real-space components of **B** are specified by a 3-D MHD equilibrium code, VMEC. Output from other equilibrium codes may be used; in particular, a subsidiary code for converting MOMCON output to conform to VMEC format is included in the discussion. Previously, output from the Chodura-Schlüter code has been used [6]. A VMEC equilibrium is described by the set of Fourier coefficients R_{mn}, Z_{mn}, and $\Psi'\lambda_{mn}$ which are defined at discrete points on a radial (s) grid, with

$$s = \Psi/\Psi_{\text{edge}} \quad . \tag{5}$$

(Hence, $\Psi' = d\Psi/ds = \Psi_{\text{edge}}$.) R and Z are the cylindrical coordinates of a given flux surface. R, Z, and ϕ are evaluated on the set of integer radial nodes $s_j = (j-1)\,\Delta s$, where $\Delta s = 1/(N_s - 1)$ and $j = 1, ..., N_s$. The quantities λ, Ψ', and ι are evaluated on the half-integer grid, $s_{j+1/2} = (s_j + s_{j+1})/2$, as described in ref. 4.

In order to calculate (R, Z, λ) at arbitrary s, a spline fit is made to all quantities. Because of the Ψ dependence of the odd poloidal harmonic components of R and Z near $\Psi = 0$, a more accurate splining can be obtained by dividing the odd-m terms by $\sqrt{\Psi}$. However, since $\Psi(s=0) = 0$, $(R_{mn}/\sqrt{\Psi})(s=0)$ and $(Z_{mn}/\sqrt{\Psi})(s=0)$ are obtained by extrapolation. Furthermore, since Ψ' and ι are given on half grids and since the spline routine sets the value outside the mesh equal to the last mesh point, Ψ' and ι are both extrapolated to $s = 0$ before splining. Thus, we can reconstruct (R, Z, λ) in the real-space cylindrical coordinate system from the splined spectral components:

$$R(s,\theta,\phi) = \frac{1}{2}\sum_n\sum_m\{1 + (-1)^m + \sqrt{\Psi}\,[1 - (-1)^m]\}R_{mn}(s)\ \cos(m\theta - n\phi) \quad , \tag{6}$$

$$Z(s,\theta,\phi) = \frac{1}{2}\sum_n\sum_m\{1 + (-1)^m + \sqrt{\Psi}\,[1 - (-1)^m]\}Z_{mn}(s)\ \sin(m\theta - n\phi) \quad , \tag{7}$$

$$\lambda(s,\theta,\phi) = \sum_n\sum_m \lambda_{mn}(s)\ \sin(m\theta - n\phi) \quad . \tag{8}$$

Then

$$\mathbf{B} = \nabla\Psi \times \{\nabla[\theta + \lambda(s,\theta,\phi)] - \iota\nabla\phi\} \quad . \tag{9}$$

Note that $\theta_o = \theta + \lambda - \iota\phi$. VMEC assumes that $\Psi_{\text{edge}} = 1$; therefore, the code magnetic field can be scaled as required, provided that the plasma pressure is also scaled appropriately.

It can be shown that the real-space components of **B** are given by

$$B^R = B^\theta\frac{\partial R}{\partial\theta} + B^\phi\frac{\partial R}{\partial\phi} \quad , \tag{10}$$

$$B^Z = B^\theta\frac{\partial Z}{\partial\theta} + B^\phi\frac{\partial Z}{\partial\phi} \quad , \tag{11}$$

$$B_{\text{tor}} = RB^\phi \quad , \tag{12}$$

where

$$B^\phi = \frac{1}{\sqrt{g}}\Psi'\left(1 + \frac{\partial\lambda}{\partial\theta}\right) \quad , \tag{13}$$

$$B^\theta = \frac{1}{\sqrt{g}}\Psi'\left(\iota - \frac{\partial\lambda}{\partial\phi}\right) \quad , \tag{14}$$

and

$$\sqrt{g} = R\left(\frac{\partial Z}{\partial s}\frac{\partial R}{\partial \theta} - \frac{\partial Z}{\partial \theta}\frac{\partial R}{\partial s}\right) \quad , \tag{15}$$

which is the Jacobian of the transformation from Cartesian coordinates to flux coordinates.

The quantities $\partial Z/\partial s$ and $\partial R/\partial s$ are obtained from Eqs. (6) and (7) by using spline fits to the quantities $R_{mn}(s)/s^m$ and $Z_{mn}(s)/s^m$ in order to increase accuracy near $s = 0$. Further, since for odd m the spline fit is done for $R_{mn}/\sqrt{\Psi}$ and $Z_{mn}/\sqrt{\Psi}$, the derivatives of these can be written

$$\frac{\partial X_{mn}}{\partial s} = \frac{\partial(X_{mn}/\sqrt{\Psi})}{\partial s}\sqrt{\Psi} + \left(\frac{X_{mn}}{\sqrt{\Psi}}\right)\frac{\partial \Psi}{\partial s} \quad (m \text{ odd}) \quad , \tag{16}$$

where $X_{mn} \equiv (R_{mn}, Z_{mn})$.

The procedure for using output from MOMCON is similar to that described previously, except that s and λ have different definitions internal to MOMCON. In VMEC, s is, as defined earlier, proportional to Ψ, whereas in MOMCON $s = \sqrt{\Psi}$. VMEC takes advantage of the packing of radial points in the outer regions of the plasma, where higher harmonics become important and where most of the stored energy exists. Thus, VMEC facilitates the energy minimization involved. With MOMCON, it is not necessary to factor the $\sqrt{\Psi}$ dependence from the Fourier coefficients.

The subroutine for calculating the real-space components of **B** from VMEC output is BCOMP. Since BCOMP has been written to accommodate VMEC output, MOMCON output must first be converted to the VMEC form in order to use it in BCOMP. A conversion program, WOUTVM, has been written to accomplish this.

4 PROGRAM DESCRIPTION AND ASSOCIATED CODES OF MAGC1

The code for evaluation of magnetic coordinates, MAGC1, has been adapted from a code of the same name developed by J. A. Rome, R. H. Fowler, T. J. Schlagel, and Hal Hancock and documented by J. A. Rome and Hal Hancock. Internal documentation for use of the code exists at Oak Ridge National Laboratory (ORNL) [7]. The code has been modified to include the subroutine BCOMP to read VMEC output and calculate $\mathbf{B}(R, Z, \phi)$ for any finite-β equilibrium. A version adapted specifically for toroidally symmetric plasmas, MAGC1T, which has some advantages over MAGC1 for such plasmas, including higher accuracy in the Fourier components, also exists. Both codes reside on the VAX network at the ORNL User Service Center. The code is written in FORTRAN IV, and the graphics is written with DISSPLA [8]. The code is divided into four parts: (1) MAGC1.FOR (or MAGC1T.FOR), the main controlling program; (2) BCOMP.FOR, for calculating the real-space $\mathbf{B}(R, Z, \phi)$ from the VMEC output; (3) MSUBS.FOR, subroutines peculiar to MAGC1; and (4) MSUBS2.FOR, general mathematical subroutines. In addition, two INCLUDE files, MAGCOM.FOR and DEFS.H, are needed. All reside in the direction [BEASLEY.MAG] on the ORNL VAX cluster. For internal readers, a listing of the program is provided in microfiche at the back of this report. Other interested readers can obtain the microfiche by writing to C. O. Beasley at ORNL.

4.1 INPUT

Input to MAGC1 consists of a logical unit 25 data file named WOUT.DAT containing information about the MHD equilibrium. Information for controlling the reading of amplitudes consists of the number of flux surfaces and the number of Fourier modes per flux surface. For each flux surface, spectral amplitudes of R, Z, and λ and the (m, n) mode numbers for the corresponding amplitudes are input. Also used are the (radial) ι and Ψ' profiles. The current version of MAGC1 accepts the WOUT.DAT file directly from the version of VMEC that resides in the direction [BEASLEY.MOMCON].

The input is accepted in the following format:

```
        READ(25,1) NTERMS, M1
        DO 10 J=1, M1
        LJ = (J-1) * NTERMS
        DO 10 MN= 1, NTERMS
        L = MN + LJ
10      READ(25,2) RMN(L), ZMN(L), ELMN(L), XM(MN), XN(MN)
        READ(25,3) (AIOTA(J), XMASS(J), VP(J), PRES(J),
          > PHIP1(J), PHI(J), BPC, BZC, SPECW(J), J=1, M1)
1       FORMAT (46X, 2I4)
2       FORMAT (3E22.14, 4E12.4)
3       FORMAT (5E22.14)
```

In these data, NTERMS is the number of m-modes times the number of n-modes, and M1 is the number of flux surfaces; RMN, ZMN, and ELMN are the amplitudes of the XMth poloidal and XNth toroidal modes of R, Z, and λ on the jth flux surface; and AIOTA and PHIP1 are the ι and Ψ' profiles, given on each flux surface. Splining of all quantities is discussed in Sect. 3.

The NAMIN-type input data file on logical unit 4, FOR004.DAT, contains the control information for running MAGC1. It is essentially the same input as that for running the vacuum case where **B** is determined from coils. Sample data for ATF follow:

```
C ALL UNITS ARE STANDARD MKS UNITS
$NAMIN
RAXIS = 2.159005          !Magnetic axis location
RBEGIN = 2.1676           !Innermost surface for analysis
ROUT = 2.254              !Outermost surface for analysis
IRUP = 1                  !Number of surfaces for analysis (max=20)
RSURF = 2.251535          !Surface if IRUP=1
STIOTA = .3               !Guess for iotabar on innermost surface;
                          !must be ≤ actual value. Lower STIOTA
                          !results in more integration time.
AN = 12.                  !Number of field periods
MINPP = 50                !Minimum number of points in puncture plot
MPERMX = 20               !Minimum allowed samples/field period
NFOUR = 13                !2^(NFOUR-1) =number samples in FFT (max=13)
IGAUS = 0                 !IGAUS=1 subtracts big peaks in spectrum
                          !to reveal smaller peaks. Normally off,
                          !and IDATOP(5,m) is used to determine
                          !cutoff level.
ETA = 4.0                 !Width of windowing Gaussian. Normally
                          !4.0. Bigger results in lower noise level;
                          !smaller results in more resolution.
ACCURC = 5.E-7            !Field line integration accuracy
ABSERR = 5.E-7            !Parameters
TOL = 1.E-6               !Tolerance of inverse transformation
                          !to find s, θ(R, Z) and vv.
TITL = 'PLA0:atf1 b2'

$
C ----------------------------------------
C
C       IDATOP(n,0) = GRAPH OPTIONS: 0=OFF 1=ON
C       n=1:IOTABAR(PSI) 2:POL. AND TOR. CURRENTS(PSI)
C         3:PLOT INTEGRAL DL/B vs THETA AND ⟨DL/B⟩(PSI)
C         4:PLOT FOURIER SPECTRUMS FOR EVERY SURFACE
C         5:PLOT PUNCTURE PLOTS FOR EVERY SURFACE
C
C       IDATOP(n,m) = OPTIONS FOR DATARR QUANTITIES
C       m=1: BMOD 2: 1/BMOD 3: R 4: Z 5: PHI-PHIBOOZER
C         6: 1/BMOD SQUARED 7: LOG BMOD
C
C       n=1: FOURIER ANALYZE 2: CLASSIFY AND PLOT Anm's
C         3: PLOT RECONSTRUCTION AND ERROR OF
C         4: SYMMETRY IN CHI 0-EVEN 1-ODD
C         5: CUTOFF FOURIER PEAKS FOR Anm's AT 1.E(negative integer)
```

```
C
$DATAIN
        NUMDAT = 6,
        IDATOP(1,0) = 1, 1, 1, 1, 1,
C
        IDATOP(1,1) = 1, 1, 1, 0, -5,
        IDATOP(1,2) = 1, 1, 1, 0, -5,
        IDATOP(1,3) = 1, 1, 1, 0, -5,
        IDATOP(1,4) = 1, 1, 1, 1, -5,
        IDATOP(1,5) = 1, 1, 1, 1, -5,
        IDATOP(1,6) = 1, 1, 1, 0, -5,
        IDATOP(1,7) = 0, 0, 0, 0, -5 $
C

$RIOTA
IOTAHI = 0              !Picks lower of ι or (AN/AL)-ι for ι
AL = 2.0                !Winding number
$END
```

4.2 OUTPUT

FOR001.DAT: WARNINGS AND ERRORS
This file contains error messages generated by the code.

FOR008.DAT: DIAGNOSTICS
Detailed diagnostics concerning the workings of the code are printed out in this file. Included are the details of how ι was found, the calculations of Boozer's I, g, and Ψ (all in mks units), and $\rho = s$, the flux-coordinate minor radius of the plasma, normalized ($\rho_{\max} = 1$). For MOMCON output, $s \propto \sqrt{\Psi}$; for VMEC, $s \propto \Psi$. Identification of all the modes, together with the "goodness" of each fit, is printed out.

FOR009.DAT: ESSENTIAL OUTPUT
This file contains Boozer's I, g, Ψ, ι, ρ, and a listing of the "good" modes.

FOR018.DAT: OUTPUT DATA
The output data set. The data are written out by the following format:

```
        WRITE(18,1) NDIM, MUP, NUMDAT, IRUP
        WRITE(18,2) (FLUX(I),TIOTAB(I),GVEC(I),BIVEC(I),I=1,MUP)
        WRITE(18,2) ((((TABALL(NT,MT,IDAT,IR), NT=1,NDIM),
          MT=1,MUP), IDAT=1, NUMDAT), IR=1,IRUP)
1       FORMAT(1H, 4I4)
2       FORMAT(1H, 5E14.7)
```

In the output data set, NDIM and MUP are the ranges of the n and m values. The m values are stored in the order

$$m = \mathrm{INT}\left(\frac{\mathrm{MT}}{2}\right)(-1)^{\mathrm{MT}}.$$

NUMDAT is the number of functions that can be analyzed, and IRUP is the total number of flux surfaces. The arrays in the second WRITE statement contain the flux, ι, and Boozer's g and I functions for each flux surface.

4.3 SUBSIDIARY CODES

Several valuable subsidiary codes exist to aid in establishing appropriate input data and in outputting data in a more usable form for DKES, for instance. These are described here.

1. BRWOUT. This program reads the WOUT.DAT file in the VMEC format described previously and outputs the contravariant cylindrical components B_R, B_Z, and B_ϕ, given the cylindrical coordinates (R, Z, ϕ) or the flux coordinates $(\rho = s, \theta, \phi)$. In addition, the program outputs the other set of coordinates. It is useful for calculating, for example, the RAXIS, RBEGIN, ROUT, and RSURF for input to MAGC1 when s is known.

2. WOUTMV. This program changes MOMCON output to VMEC output for use in MAGC1.

3. READAMN. This program calculates various B-field components from FOR018.DAT output and catalogs all spectral components of B^{-1}, B^{-2}, and $\sqrt{g}$ for use in DKES. Here, B is the magnitude of B, and $\sqrt{g}$ is the Jacobian $[\sqrt{g} = (g + \iota I)/B^2]$.

4. RDTOKAMN. This program does the same as item 3, but for toroidally symmetric systems. It is much more practical for such systems. It also creates an input data file for the Fourier components of the needed components of **B** which can be read directly by the version of DKES applicable to toroidally symmetric plasmas (tokamaks).

5 EXAMPLE: FINITE-β ATF

We show here a sample calculation for ATF for (averaged) $\beta = 0$ and $\beta = 0.02$. In this example, the ι profile was held fixed, while the mass profile was changed to achieve the correct β in order to compare neoclassical transport for the same ι on a given flux surface at a given radius s.

Figure 1 shows sets of puncture plots at $\phi = 0$ and $\phi = \pi/12$ (the number of toroidal field periods in the ATF is 12). Notice the outward (Shafranov) shift of the nested flux surfaces as β becomes larger. The reconstruction of the flux surfaces calculated from (R, Z), superimposed on the flux surfaces, is shown in Fig. 2 for $\phi = 0$.

Figure 3 shows the details of B in Boozer coordinates for $\rho = 0.9$ as examples of the graphic output of MAGC1. Parts (a), (b), and (c) show, respectively, the Fourier spectrum, modes, and reconstruction (with error shown) of B for $\beta = 0$, and parts (d), (e), and (f) show the same graphs for $\beta = 0.02$. Similar output can be obtained for $1/B_{\text{Boozer}}$, $1/B^2_{\text{Boozer}}$, R_{Boozer}, Z_{Boozer}, and $\phi - \phi_{\text{Boozer}}$. As detailed previously, the FOR018.DAT file contains numerical output for these same Fourier coefficients suitable for input into DKES.

Input data for the $\beta = 2$ case are listed in Sect. 4.

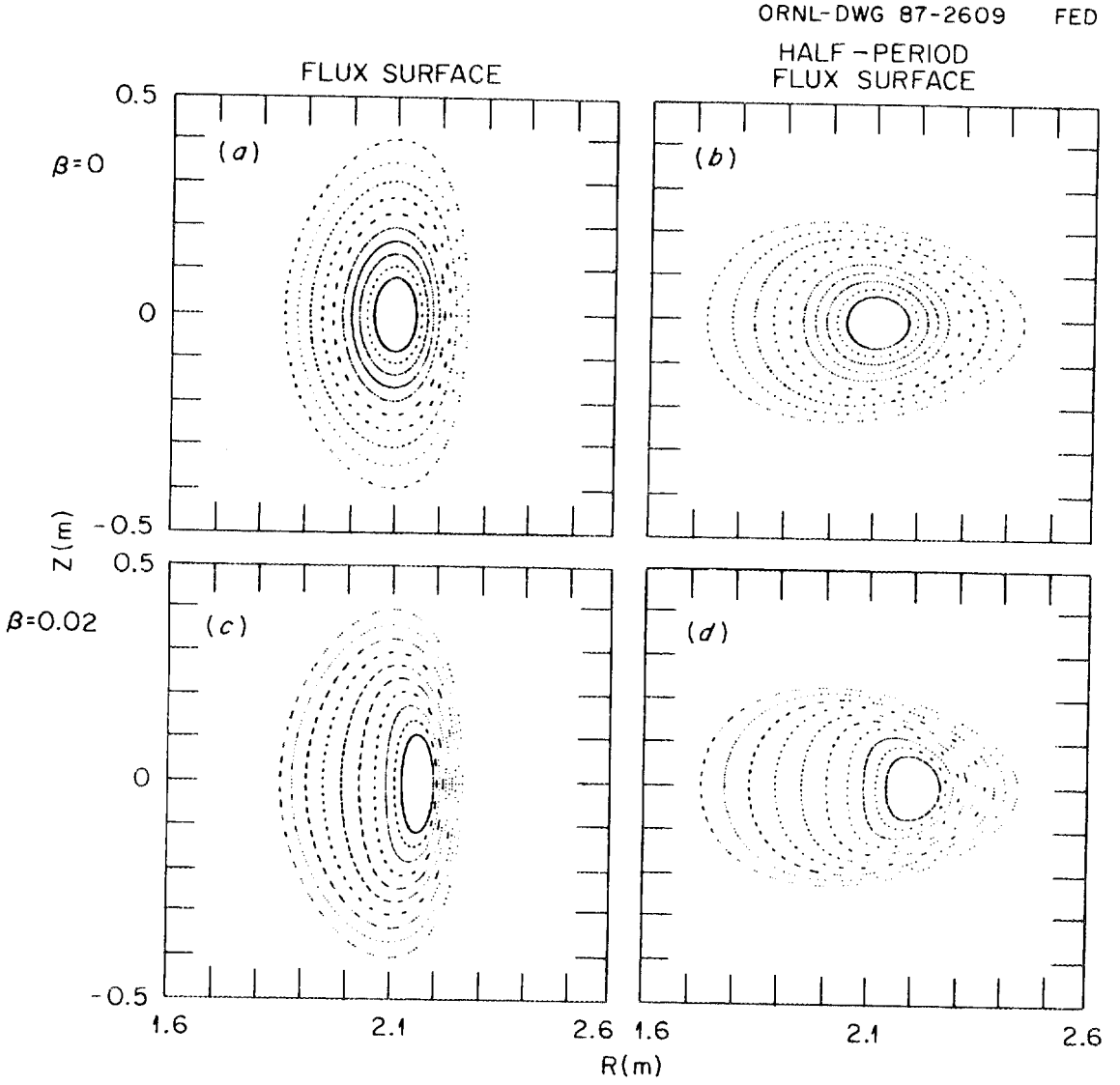

Figure 1. Flux surfaces for ATF for $\beta = 0$ and $\beta = 0.02$.

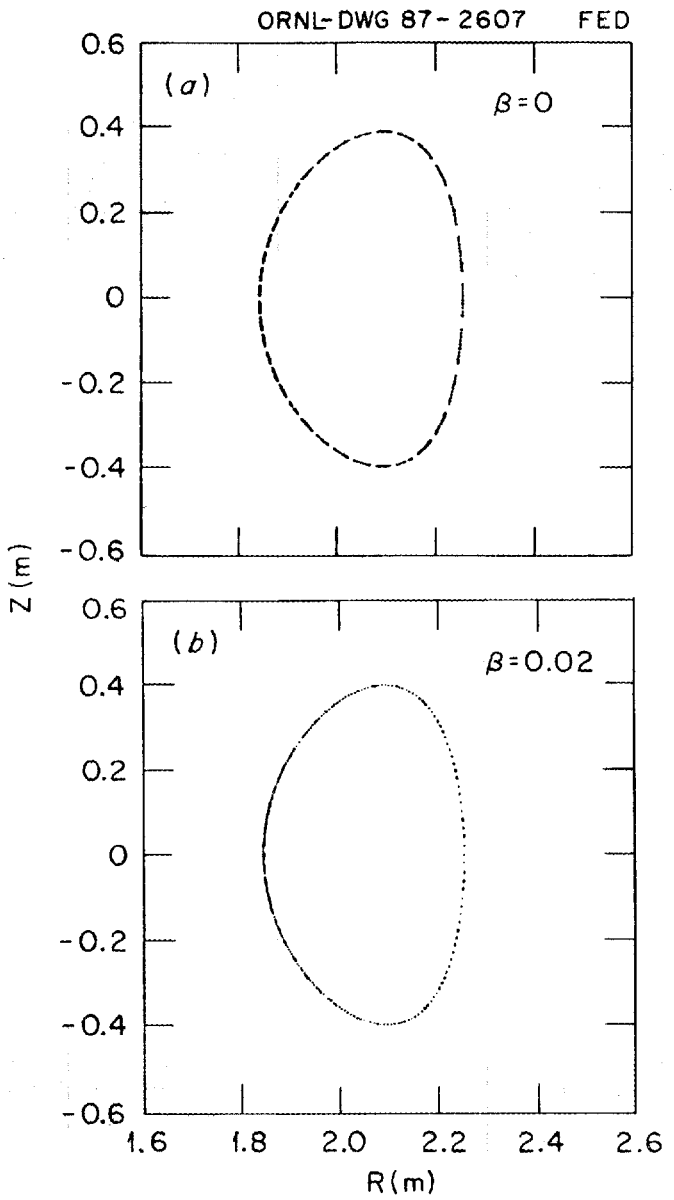

Figure 2. Reconstruction of an outer flux surface from Fourier components in Boozer coordinates for $\beta = 0$ and $\beta = 0.02$.

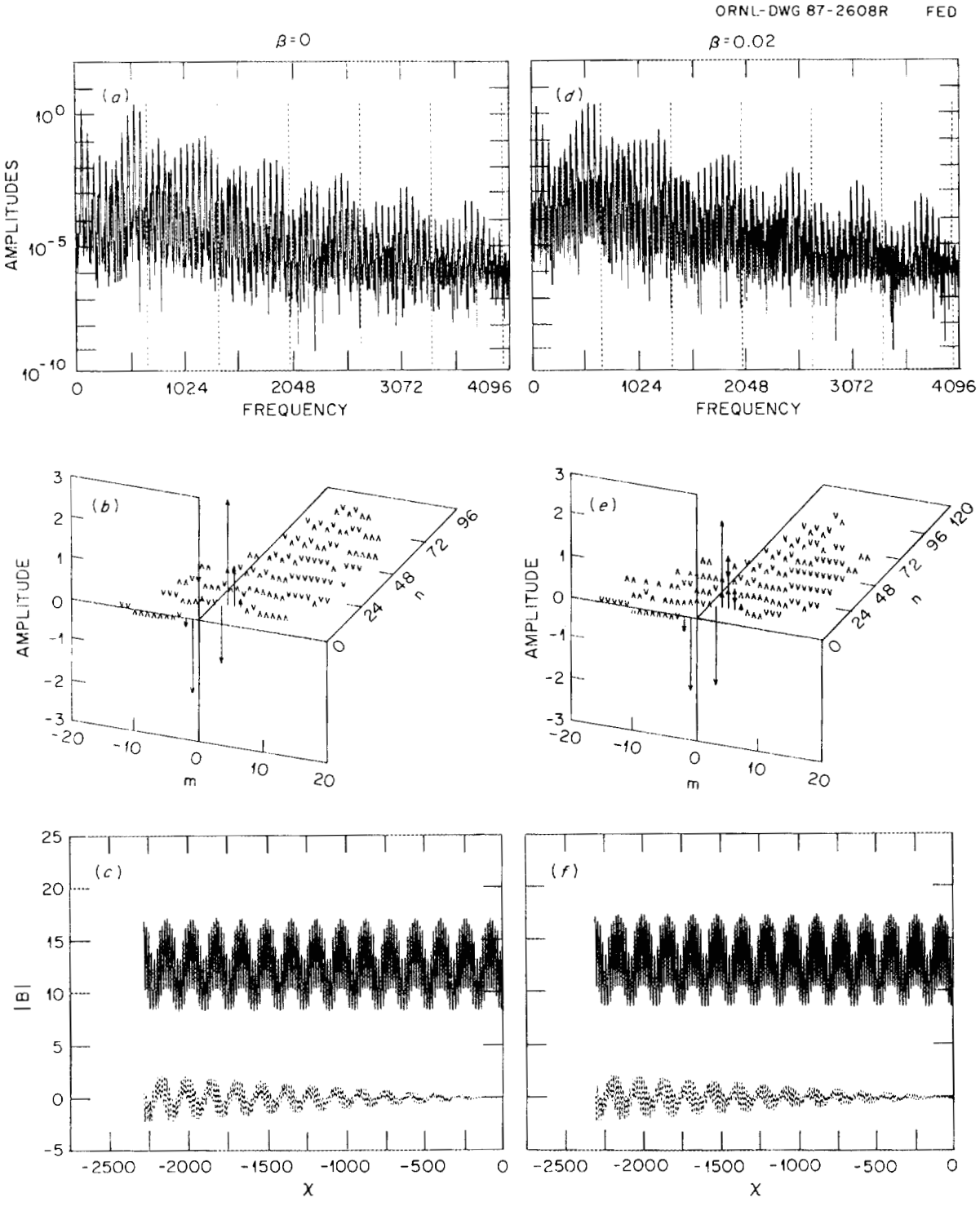

Figure 3. Fourier spectra of B, Fourier harmonics of B, and $|B|(\chi)$ reconstruction in Boozer variables for ATF for $\beta = 0$ [Parts (a), (b), and (c), respectively] and for $\beta = 0.02$ [Parts (d), (e), and (f), respectively].

6 CONCLUSION

Given the ideal MHD equilibrium for any low- or finite-β plasma, the method for converting the VMEC or MOMCON output to magnetic field quantities in Boozer coordinates has been described. The method of obtaining $\mathbf{B}(R, Z, \phi)$ from this output by using the BCOMP routine was described, and use of this real-space $\mathbf{B}$ to obtain the Boozer $\mathbf{B}$ was outlined. Two examples of zero- and finite-β ATF were shown. Availability of these codes in the Fusion Energy Division at ORNL provides a practical means of calculating any Boozer magnetic field quantities.

REFERENCES

[1] S. P. Hirshman, K. C. Shaing, W. I. van Rij, J. C. O. Beasley, and E. C. Crume, *Phys. Fluids* **29**, 2951 (1986).

[2] A. H. Boozer, *Phys. Fluids* **23**, 904 (1980).

[3] S. P. Hirshman and J. C. Whitson, *Phys. Fluids* **26**, 3553 (1983).

[4] S. P. Hirshman et al., *Comput. Phys. Commun.* **43**, 143 (1986).

[5] G. Kuo-Petravic, A. H. Boozer, J. A. Rome, and R. H. Fowler, *J. Comput. Phys.* **51**, 261 (1983).

[6] K.-C. Shaing and S. A. Hokin, *Phys. Fluids* **26**, 2136 (1983).

[7] J. A. Rome, *MAGC1 User's Guide*, Fusion Energy Division Theory Section Memorandum 86/23, Oak Ridge Natl. Lab., Martin Marietta Energy Systems, Inc., 1986.

[8] *DISSPLA — Display Integrated Software System and Plotting Language*, Integrated Software Systems Corporation, San Diego, California, 1986.

ORNL/TM-10222
Dist. Category UC-20 g

INTERNAL DISTRIBUTION

1–2. S. E. Attenberger
3–7. C. O. Beasley
8. B. A. Carreras
9. R. A. Dory
10. M. L. Givens
11. J. A. Harris
12. C. L. Hedrick
13–14. S. P. Hirshman
15. J. T. Hogan
16. W. A. Houlberg
17. H. C. Howe
18. G. H. Neilson
19. Y-K. M. Peng
20–21. J. A. Rome
22. J. Sheffield
23. J. S. Tolliver
24. N. A. Uckan
25–26. Laboratory Records Department
27. Laboratory Records, ORNL-RC
28. Document Reference Section
29. Central Research Library
30. Fusion Energy Division Library
31–32. Fusion Energy Division Publications Office
33. ORNL Patent Office

EXTERNAL DISTRIBUTION

34. Office of the Assistant Manager for Energy Research and Development, U.S. Department of Energy, Oak Ridge Operations Office, P. O. Box E, Oak Ridge, TN 37831
35. J. D. Callen, Department of Nuclear Engineering, University of Wisconsin, Madison, WI 53706-1687
36. J. F. Clarke, Director, Office of Fusion Energy, Office of Energy Research, ER-50 Germantown, U.S. Department of Energy, Washington, DC 20545
37. R. W. Conn, Department of Chemical, Nuclear, and Thermal Engineering, University of California, Los Angeles, CA 90024
38. S. O. Dean, Fusion Power Associates, 2 Professional Drive, Suite 248, Gaithersburg, MD 20879
39. H. K. Forsen, Bechtel Group, Inc., Research Engineering, P. O. Box 3965, San Francisco, CA 94105
40. J. R. Gilleland, GA Technologies, Inc., Fusion and Advanced Technology, P.O. Box 81608, San Diego, CA 92138
41. R. W. Gould, Department of Applied Physics, California Institute of Technology, Pasadena, CA 91125
42. R. A. Gross, Plasma Research Laboratory, Columbia University, New York, NY 10027
43. D. M. Meade, Princeton Plasma Physics Laboratory, P.O. Box 451, Princeton, NJ 08544
44. M. Roberts, International Programs, Office of Fusion Energy, Office of Energy Research, ER-52 Germantown, U.S. Department of Energy, Washington, DC 20545
45. W. M. Stacey, School of Nuclear Engineering and Health Physics, Georgia Institute of Technology, Atlanta, GA 30332
46. D. Steiner, Nuclear Engineering Department, NES Building, Tibbetts Avenue, Rensselaer Polytechnic Institute, Troy, NY 12181

47. R. Varma, Physical Research Laboratory, Navrangpura, Ahmedabad 380009, India
48. Bibliothek, Max-Planck Institut fur Plasmaphysik, D-8046 Garching, Federal Republic of Germany
49. Bibliothek, Institut fur Plasmaphysik, KFA, Postfach 1913, D-5170 Julich, Federal Republic of Germany
50. Bibliotheque, Centre de Recherches en Physique des Plasmas, 21 Avenue des Bains, 1007 Lausanne, Switzerland
51. F. Prevot, CEN/Cadarache, Departement de Recherches sur la Fusion Controlee, F-13108 Saint-Paul-lez-Durance Cedex, France
52. Documentation S.I.G.N., Departement de la Physique du Plasma et de la Fusion Controlee, Centre d'Etudes Nucleaires, B.P. 85, Centre du Tri, F-38031 Grenoble, France
53. Library, Culham Laboratory, UKAEA, Abingdon, Oxfordshire, OX14 3DB, England
54. Library, FOM-Instituut voor Plasma-Fysica, Rijnhuizen, Edisonbaan 14, 3439 MN Nieuwegein, The Netherlands
55. Library, Institute of Plasma Physics, Nagoya University, Nagoya 464, Japan
56. Library, International Centre for Theoretical Physics, P.O. Box 586, I-34100 Trieste, Italy
57. Library, Laboratorio Gas Ionizatti, CP 56, I-00044 Frascati, Rome, Italy
58. Library, Plasma Physics Laboratory, Kyoto University, Gokasho, Uji, Kyoto, Japan
59. Plasma Research Laboratory, Australian National University, P.O. Box 4, Canberra, A.C.T. 2000, Australia
60. Thermonuclear Library, Japan Atomic Energy Research Institute, Tokai Establishment, Tokai-mura, Naka-gun, Ibaraki-ken, Japan
61. G. A. Eliseev, I. V. Kurchatov Institute of Atomic Energy, P.O. Box 3402, 123182 Moscow, U.S.S.R.
62. V. A. Glukhikh, Scientific-Research Institute of Electro-Physical Apparatus, 188631 Leningrad, U.S.S.R.
63. I. Shpigel, Institute of General Physics, U.S.S.R. Academy of Sciences, Ulitsa Vavilova 38, Moscow, U.S.S.R.
64. D. D. Ryutov, Institute of Nuclear Physics, Siberian Branch of the Academy of Sciences of the U.S.S.R., Sovetskaya St. 5, 630090 Novosibirsk, U.S.S.R.
65. V. T. Tolok, Kharkov Physical-Technical Institute, Academical St. 1, 310108 Kharkov, U.S.S.R.
66. Library, Academia Sinica, P.O. Box 3908, Beijing, China (PRC)
67. D. Crandall, Experimental Plasma Research Branch, Division of Development and Technology, Office of Fusion Energy, Office of Energy Research, ER-542 Germantown, U.S. Department of Energy, Washington, DC 20545
68. N. A. Davies, Office of the Associate Director, Office of Fusion Energy, Office of Energy Research, ER-51 Germantown, U.S. Department of Energy, Washington, DC 20545

69. D. B. Nelson, Director, Division of Applied Plasma Physics, Office of Fusion Energy, Office of Energy Research, ER-54 Germantown, U.S. Department of Energy, Washington, DC 20545

70. E. Oktay, Division of Confinement Systems, Office of Fusion Energy, Office of Energy Research, ER-55 Germantown, U.S. Department of Energy, Washington, DC 20545

71. W. Sadowski, Fusion Theory and Computer Services Branch, Division of Applied Plasma Physics, Office of Fusion Energy, Office of Energy Research, ER-541 Germantown, U.S. Department of Energy, Washington, DC 20545

72. P. M. Stone, Fusion Systems Design Branch, Division of Development and Technology, Office of Fusion Energy, Office of Energy Research, ER-532 Germantown, U.S. Department of Energy, Washington, DC 20545

73. J. M. Turner, International Programs, Office of Fusion Energy, Office of Energy Research, ER-52 Germantown, U.S. Department of Energy, Washington, DC 20545

74. R. E. Mickens, Atlanta University, Department of Physics, Atlanta, GA 30314

75. M. N. Rosenbluth, RLM 11.218, Institute for Fusion Studies, University of Texas, Austin, TX 78712

76. Duk-In Choi, Department of Physics, Korea Advanced Institute of Science and Technology, P.O. Box 150, Chong Ryang-Ri, Seoul, Korea

77. Theory Department Read File, c/o D. W. Ross, University of Texas, Institute for Fusion Studies, Austin, TX 78712

78. Theory Department Read File, c/o R. C. Davidson, Director, Plasma Fusion Center, NW 16-202, Massachusetts Institute of Technology, Cambridge, MA 02139

79. R. R. Parker, Plasma Fusion Center, NW 16-288, Massachusetts Institute of Technology, Cambrige, MA 02139

80. Theory Department Read File, c/o R. White, Princeton Plasma Physics Laboratory, P.O. Box 451, Princeton, NJ 08544

81. Library of Physics Department, University of Ioannina, Ioannina, Greece

82. Theory Department Read File, c/o L. Kovrizhnykh, Lebedev Institute of Physics, Academy of Sciences, 53 Leninsky Prospect, 117924 Moscow, U.S.S.R.

83. Theory Department Read File, c/o B. B. Kadomtsev, I. V. Kurchatov Institute of Atomic Energy, P.O. Box 3402, 123182 Moscow, U.S.S.R.

84. Theory Department Read File, c/o T. Kamimura, Institute of Plasma Physics, Nagoya University, Nagoya 464, Japan

85. Theory Department Read File, c/o C. Mercier, Departemente de Recherches sur la Fusion Controlee, B.P. No. 6, F-92260 Fontenay-aux-Roses (Seine), France

86. Theory Department Read File, c/o T. E. Stringer, JET Joint Undertaking, Culham Laboratory, Abingdon Oxfordshire, OX14 3DB, England

87. Theory Department Read File, c/o R. Briscoe, Culham Laboratory, Abingdon, Oxfordshire OX14 3DB, England

88. Theory Department Read File, c/o D. Biskamp, Max-Planck-Institut fur Plasmaphysik, D-8046 Garching, Federal Republic of Germany

89. Theory Department Read File, c/o T. Takeda, Japan Atomic Energy Research Institute, Tokai Establishment, Tokai-mura, Naka-gun, Ibaraki-ken, Japan

90. Theory Department Read File, c/o J. Greene, GA Technologies, Inc., P.O. Box 81608, San Diego, CA 92138

91. Theory Department Read File, c/o L. D. Pearlstein, L-630, Lawrence Livermore National Laboratory, P.O. Box 5511, Livermore, CA 94550

92. Theory Department Read File, c/o R. Gerwin, CTR Division, Los Alamos National Laboratory, P.O. Box 1663, Los Alamos, NM 87545

93. R. J. Hawryluk, Princeton Plasma Physics Laboratory, P.O. Box 451, Princeton, NJ 08544

94. D. E. Post, Princeton Plasma Physics Laboratory, P.O. Box 451, Princeton, NJ 08544

95. M. G. Bell, Princeton Plasma Physics Laboratory, P.O. Box 451, Princeton, NJ 08544

96. S. C. Jardin, Princeton Plasma Physics Laboratory, P.O. Box 451, Princeton, NJ 08544

97. R. G. Bateman, Princeton Plasma Physics Laboratory, P.O. Box 451, Princeton, NJ 08544

98. C. K. Phillips, Princeton Plasma Physics Laboratory, P.O. Box 451, Princeton, NJ 08544

99. D. R. Mikkelsen, Princeton Plasma Physics Laboratory, P.O. Box 451, Princeton, NJ 08544

100. S. Ejima, GA Technologies, Inc., P.O. Box 85608, San Diego, CA 92138

101. A. G. Kellman, GA Technologies, Inc., P.O. Box 85608, San Diego, CA 92138

102. L. L. Lao, GA Technologies, Inc., P.O. Box 85608, San Diego, CA 92138

103. G. A. Emmert Department of Nuclear Engineering, University of Wisconsin, Madison, WI 53706-1687

104. P. R. Thomas, JET Joint Undertaking, Culham Laboratory, Abingdon Oxfordshire, OX14 3DB, England

105. M. L. Watkins, JET Joint Undertaking, Culham Laboratory, Abingdon Oxfordshire, OX14 3DB, England

106–221. Given distribution according to TIC-4500, Magnetic Fusion Energy (Category Distribution UC-20g, Theoretical Plasma Physics)